Journal of Physics: Condensed Matter

PAPER

The role of defects in the physical properties of mechanically activated $PbTiO_3$ ferroelectrics

IOP Publishing Journal of Physics: Condensed Matter
J. Phys.: Condens. Matter **31** (2019) 135402 (5pp) https://doi.org/10.1088/1361-648X/aafebe

The role of defects in the physical properties of mechanically activated $PbTiO_3$ ferroelectrics

K G Abdulvakhidov[1,5], M A Sirota[2], A P Budnyk[1], T A Lastovina[1], B K Abdulvakhidov[3], S A Sadykov[3], P S Plyaka[4] and A V Soldatov[1]

[1] The Smart Materials International Research Institute, Southern Federal University, Rostov-on-Don, Russia
[2] Don State Technical University, Rostov-on-Don, Russia
[3] Dagestan State University, Makhachkala, Russia
[4] Southern Scientific Centre, Russian Academy of Sciences, Rostov-on-Don, Russia

E-mail: phys.kam@mail.ru

Received 26 October 2018, revised 24 December 2018
Accepted for publication 15 January 2019
Published 1 February 2019

Abstract

In this work a multi-technique characterization was performed for the first time to trace the influence of structural defects on the physical properties of $PbTiO_3$ ferroelectrics. The structural defects were generated by the mechanical activation in the pressure range of 40–320 MPa, by combining a uniaxial strain with a shear deformation in the Bridgman anvils. The induced defectivity of $PbTiO_3$ was assessed via calculation of unit cell parameters, estimation of the regions of coherent scattering and analysis of micro-deformations. The Debye characteristic temperature, the static mean-square displacement, the Debye–Waller isotropic factor, the vibrational spectra and dielectric properties of the activated $PbTiO_3$ ceramics are presented. The high-quality $PbTiO_3$ ceramics was prepared without modifiers, hence, changing the concentration of structural defects via mechanical activation constitutes a chemically clean method for fine tuning of the dielectric properties of $PbTiO_3$.

Keywords: $PbTiO_3$, mechano-activation, defects, Bridgman anvils

Supplementary material for this article is available online

(Some figures may appear in colour only in the online journal)

1. Introduction

The classical ferroelectric lead(II) titanate (LT) is one of the frequently used modifiers to adjust physical properties of perovskites for some practical applications [1–4]. The $PbTiO_3$ composition occupies a far-right position in the x-T phase diagram of the $PbZr_{1-x}Ti_xO_3$ solid solutions, where x is the titanium concentration in the alloy and T is the temperature of the phase transition. By varying the LT concentration in solid solution, one may influence the resulting phase transition temperature, piezomodules, vibrational spectra and dielectric properties, dynamic and structural parameters of the crystal lattice [5–9]. This method became a common approach in ceramic technology.

It is rather difficult to prepare the LT ceramics without the use of dopants [10]. Sintering of powder forms the grains from hundreds of nm to tens of μm. While cooling down, a ceramic sample may fracture during the first phase transition from the paraelectric cubic phase to the ferroelectric tetragonal one (at ~490 °C), releasing inhomogeneous deformation via mechanical stress. That is typically observed for the compacts with prevalence of micro-sized grains, where the damper effect due to an interlaying amorphized $PbTiO_3$ is negligible. The

[5] The Smart Materials International Research Institute, Southern Federal University, Sladkova 178/24, 344090, Rostov-on-Don, Russia.

uniform deformation parameter, δ, given as $c/a - 1$ (where c and a are the unit cell parameters), equals ~0.063 for tetragonal LT at room temperature. By reducing the size of grains until a sub-micrometer scale, one may observe and exploit the deviation in electrophysical and dynamic properties arising due to the classical dimensional effect.

Ferroelectric powders are prepared by either grinding or mechanochemistry using planetary mills. Grinding as a process forms new surfaces, generates heat, dislocations and point defects, changes interplanar distances and coupling angles, forms metastable polymorphs and promotes chemical interactions. The mechanical mixing of the initial oxides brings them to form a composite. This process is accompanied by relaxation of mechanical energy via different mechanisms. Powder can be subsequently fused into ceramics by high temperature sintering. It is usually a two-step thermo-physical and chemical process, which induces diffusion and annealing of the defects in the crystalline structure. Even a modest amount of remaining point defect significantly alters the physical properties of ferroelectrics. Unlike in single crystals, it is not possible to estimate quantitatively the concentration of point defects in powder and ceramic samples, therefore, all judgments are rather qualitative in nature.

Earlier, we proposed a method for a noticeable modification of physical properties of $PbZr_{0.56}Ti_{0.44}O_3$ piezoceramics by changing the concentration of dislocations and point defects without altering the chemical composition [11]. In the present work, we extend the adopted approach to the LT materials by changing the concentration of structural defects via mechanical stress. For this purpose, the LT powder was compacted in the rotating Bridgman anvils to experience a hydrostatic-type stress, which combines an applied unidirectional force with the shear strain. We will focus on behavior of dielectric properties of samples as powders and compacts because of their relevance for typical applications of LT-based materials.

2. Methods

A preparation method was similar to previously published [11–15]. In brief, the metal oxides were mechanically mixed for 2 h and compacted into a tablet. Some $PbZrO_3$ was added to compensate a partial loss of PbO subliming at high temperatures. The powder was sintered at 1420 K for 2 h and furnace was left cooling down naturally. The tablets were ground into a fine powder, which was labeled as the 'starting' sample. The crystalline phase of the batches was controlled with x-ray diffraction (XRD) measurements confirming their reproducibility. The representative electronic micrograph and XRD pattern are presented in figure S1a (supplemental data (stacks.iop.org/JPhysCM/31/135402/mmedia)).

The mechanical activation was performed in the Bridgman anvils, where the powder was confined in a metallic ring, positioned between the anvils. The lower anvil was rotating at a low angular velocity of $\Omega = 0.3$ rad min^{-1}. The mechanical load, P, ranging from 80 to 320 MPa with a 40 MPa step was applied. Each 'activated' sample was formed by gathering 7 portions of powder experienced the same stress. The representative electronic micrograph and XRD pattern for the sample experienced the applied pressure of 240 MPa are presented in figure S1(b).

The XRD patterns were measured on an HZG-4B diffractometer with Cu Kα emission in the Bragg–Brentano geometry. The Rietveld refinement analysis was performed in Powder Cell 2.3 software [16]. The XRD measurements of the integral intensities of the (1 1 0) and (2 2 0) reflections, $I_{(1\,1\,0)}$ and $I_{(2\,2\,0)}$, in the paraelectric cubic phase were performed at 773 and 873 K by using a high-temperature home-made accessory for the diffractometer. The Fourier-transform infrared (FTIR) spectra were recorded on a FSM-1202 spectrometer. For electrophysical measurements powders were compacted altogether and sintered into ceramic discs at 1370 K for 1 h. Dielectric spectra were measured on an E7-20 immittance meter. Other experimental details are given in supplemental data.

3. Results and discussion

All the prepared 'starting' powders regardless the batch demonstrated a crystalline phase pattern of $PbTiO_3$ tetragonal phase, evidencing the absence of impurities (see figure S1(a)). The spatial symmetry group was defined as $P4mm$. The pressure range of 80–320 MPa was chosen to create a sufficient mechanical stress for generation of structural defects, however, avoiding the substantial amorphization and uncontrolled phase transformation. The XRD profiles of the samples after mechanical stress (see figure S2) exhibit an elevated background level, broadened peaks, and suppressed integrated intensities. These changes reflect the presence of both the static and dynamic distortions of the crystal lattice. As can be seen from figure 1(a) the values of lattice parameters a and c (united by polynomial eyeguides) appear increasing and oscillating under amplifying pressure.

The applied mechanical stress should influence the size of the coherent scattering region, D, and to introduce microdeformations, estimated as $\Delta d/d$. Under these conditions the classical Debye-Scherrer formula is not applicable, therefore, both D and $\Delta d/d$ values will be evaluated from the FWHM values by the approximation method. The results are shown in figure 1(b). The D parameter decreases monotonically up to 160 MPa and turns to this value after eventual increase at 200 MPa. At the same pressure the growth of the $\Delta d/d$ parameter is impaired with lower values. This mutual deviation in a steady behavior of both characteristic parameters may suggest the presence of a recrystallization process favored by the dynamic diffusion due to mechanoactivation [17].

Since the role of screw dislocations in the broadening of XRD profiles due to experienced mechanical stress is practically insignificant, we can assume of dealing mainly with the edge dislocations; supposing their chaotical distribution, the dislocation density, ρ_D, can be calculated as [18]:

$$\rho_D = 3nD^{-2}, \quad (1)$$

where the $n = 1$ corresponds to a dislocation grid with dislocations situated at the edges, ensuring the maximal distance

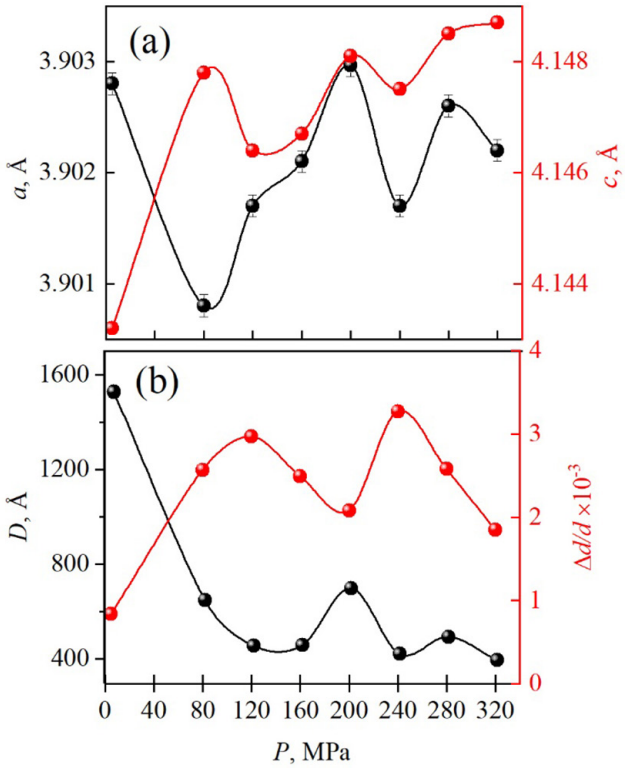

Figure 1. Stress-induced changes in the unit cell parameters, a and c, (a) and the size of the coherent scattering regions, D, and micro-deformations, $\Delta d/d$, (b) of $PbTiO_3$ powders.

Table 1. Density of dislocations in $Pb(Zr_{0.56}Ti_{0.44})O_3$.

P, MPa	0	80	120	160	200	240	280	320
$\rho_D \cdot 10^9$, cm^{-2}	13	76	162	205	179	162	134	127

between the dislocations and minimal mutual interactions, D is the coherent scattering region. The calculated values are presented in table 1.

In order to see how mechanical stress affects the thermally-driven displacement of ions in solid solution from their ground-state equilibrium positions, we estimated the root-mean-square amplitude, $\bar{U}^2$, from the (1 1 0) and (2 2 0) reflections measured at 775 K and 875 K in the nonpolar cubic phase (figure S3), according to formula:

$$\bar{U}^2 = \frac{3a^2}{4\pi\,(N_2 - N_1)} \ln\left[\frac{\left(\frac{I_{(1\,1\,0)}}{I_{(2\,2\,0)}}\right)_{\text{activated}}}{\left(\frac{I_{(1\,1\,0)}}{I_{(2\,2\,0)}}\right)_{\text{starting}}}\right], \qquad (2)$$

where a is the lattice parameter, N_1 and N_2 are the sums of the squares of the Miller indices, $I_{(110)}$ and $I_{(220)}$ are the integral intensities of the (1 1 0) and (2 2 0) reflections.

The $\bar{U}^2$ values for 'activated' samples measured at two temperatures are presented in figure 2. The two sets oscillate to a different extent with increasing applied pressure suggesting that 'activated' samples are in various metastable states. At 775 K the diffusion processes are not yet manifested evidently while rising temperature on 100 K leads to an increase in the diffusion coefficient, thus, smoothing the effect from metastable states. These conditions are favorable for

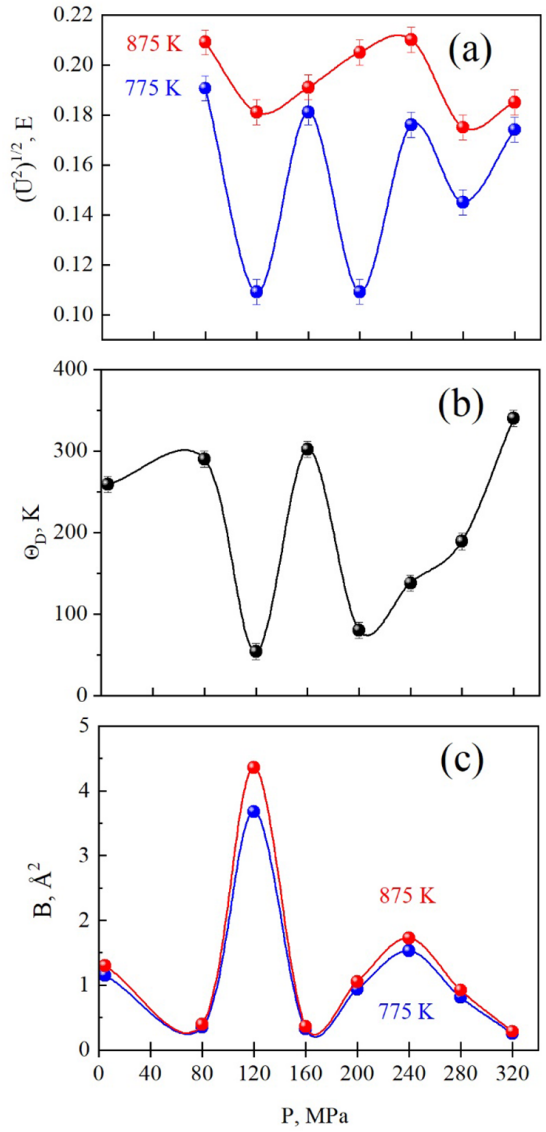

Figure 2. The root-mean-square amplitude (a), the Debye characteristic temperature Θ_D (b) and the Debye–Waller factor B (c) for the $PbTiO_3$ samples after applied pressures.

partial 'healing' of dislocations, migration of generated point defects to grain boundaries and to vacant crystallographic positions in unit cells. All that improves the crystal lattice; as the contribution from static displacements decreases, the dynamic ones play the dominant role in $\bar{U}^2$. However, even after sintering some ions still remain displaced and presence of corresponding vacancies affects the charge state of the unit cell as well as the transport and thermodynamic properties of the crystallites. The majority of impurities, being foreign to a given crystal lattice, also reach the grain's surface. Therefore, mechanoactivation of real solids often leads to suppression of electrical conductivity, for example, as in [19].

As it is known, in the transition from macrocrystals to objects of the mesoscopic scale, the amplitude of atomic vibrations increases, the characteristic Debye temperature decreases, the isotropic Debye–Waller factor increases, the melting temperature decreases, etc. However, these changes in properties are valid only under the condition that diffusion

processes are absent between the particles, and they are in a thermodynamic equilibrium state and particles are ordered (without vacancies and impurities). In our case, as can be seen from the results set forth above, not all the listed conditions are met.

Next, consider how applied pressure will affect dynamic parameters of the crystal lattice. We calculate the characteristic Debye temperature, Θ_D, and the isotropic thermal Debye–Waller factor, B, by assuming the $PbTiO_3$ crystal lattice as an infinite medium where ions in the para-phase oscillate independently and isotropically. Such assumption permits to process the experimental diffraction profiles regardless the role of the diffusion background arising between the Bragg peaks due to the thermal displacement of ions [20, 21]. The texture of each sample was accounted by estimating Θ_D via the ratio of the intensities of XRD profiles measured at two fixed temperatures [22] according to formula:

$$\ln \frac{I_{T_1}}{I_{T_2}} = 12 \frac{h^2}{m_a \Theta_D k} \left[\left(\frac{F(x_1)}{x_1} \right) - \left(\frac{F(x_2)}{x_2} \right) \right] S^2, \quad (3)$$

where $x_1 = \theta_D/T_1, x_2 = \theta_D/T_2$, h is the Planck constant, k is the Boltzmann constant, $F(x)$ is the Debye function, $m_a = \sum n_i m_i / \sum m_i$ is the average atomic mass, n_i is the number of atoms in the cell, $S = \sin \upsilon/\lambda$.

The B values were calculated from obtained Θ_D values for two temperatures according to formula:

$$B(T) = 6T \frac{h^2}{m_a \Theta_D k^2} \left[F(x) + \frac{x}{4} \right]. \quad (4)$$

The dependencies of Θ_D and B on the applied pressures are shown in figures 2(b) and (c). The former does not present a strict-correlated pattern, supposedly, being a fruit of different impacts from $m_a\Theta_D$ entities, which are proportional to restoring forces for ions shifted from the equilibrium positions due to thermal oscillations. The temperature-driven dynamic deviations from equilibrium position and static displacements of ions caused by the presence of dislocations and point defects around their equilibriums all influence the B value. Its linear growth with the temperature rise is expected, according to equation (4). This would be the case on condition of $T \gg \Theta_D$, which is fulfilled at $P = 120$ MPa, where Θ_D has a minimum value.

The phonon spectrum of the crystal lattice is known to be sensitive to crystallites size and defectivity. FTIR spectra were collected at room temperature after each step of mechanical activation. All of them contain a complex vibrational band extending from about 800 to 450 cm^{-1}, with a center situated at about 560 cm^{-1} (see figure S4). The band is asymmetric, with a high-frequency tail featuring two components at 767 and 701 cm^{-1}. This characteristic band is formed by Ti–O stretching vibrations of TiO_6 octahedron [23]. Already after 80 MPa pressure, the maximum of the main band shifts from 550 to 574 cm^{-1} and becomes more intense and well resolved. Its maximum remains at 574 cm^{-1} along all sequence of strain-tests, allowing to follow the change of its absolute intensity with applied pressure, as presented in figure 3(a). The overall trend of the change resembles that of micro-deformations (see $\Delta d/d$ curve in figure 1(b), just having a 40 MPa delay.

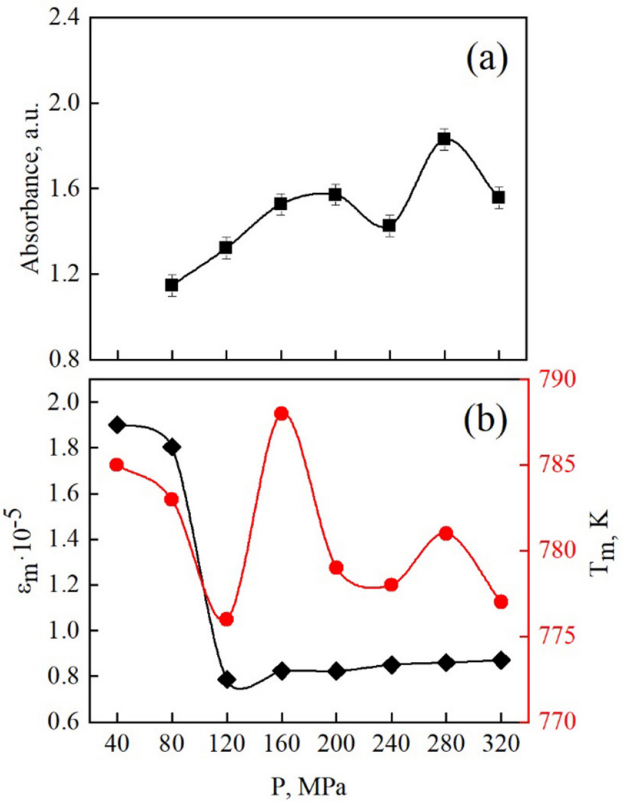

Figure 3. The dependences of the IR band intensity at 574 cm^{-1}, corresponding to the Ti–O stretching mode (a), of the dielectric constant at a maximum of ε_m and the corresponding temperatures T_m (b) of ceramic samples $PbTiO_3$ on the value of the activation pressure.

The most important parameters of ferroelectrics are the permittivity ε and the tangent of the dielectric loss angle $\tan\delta$, which very often determine their practical application as functional materials. Usually pure $PbTiO_3$ single crystals are characterized by a clear first-order phase transition, and it is observed at a Curie temperature $T_c = 763$ K. However, for the measurement methods of ε, where there is no compensation for the high conductivity of $PbTiO_3$, it is difficult to clearly record such a phase transition, but it can be observed by anomalies in the dependence of $\tan\delta(T)$, lagging T_c by about 10–15 K. The dependences of $\varepsilon(T)$ and $\tan\delta(T)$ for two ceramic samples obtained from the 'starting' and 'activated' powders are shown in figure S5. As it can be seen, mechano-activation of the $PbTiO_3$ powder at 240 MPa leads to decrease of T_m for ceramics for about 7 K.

Figure 3(b) shows the dependences of the dielectric constant at a maximum of ε_m and the corresponding temperatures T_m of ceramic samples $PbTiO_3$ on the value of the activation pressure. Starting at a pressure of 120 MPa, the dielectric constant ε_m of 'activated' samples decreases more than twice as compared to 'starting' sample, the phase transitions are washed out and the temperature T_m changes nonmonotonically depending on the pressures, powder activation $PbTiO_3$. The study of the dielectric hysteresis of ceramic samples on the Sawyer-Tower showed that the loops do not saturate even at a field strength of 8 kV cm^{-1}, which is due to the structural defectiveness and the difficulty in switching the polarization.

4. Conclusion

In summary, this work presents the results of an experimental study about mechanoactivation of $PbTiO_3$ in the Bridgman anvils. This treatment leads to formation of nano- and micro-particles, which are in different meta-stable states. At this scale size-driven effects occur more pronouncedly, affecting structural properties, lattice dynamics and dissipative properties. By applying a quasi-hydrostatic mechanical load in 80–320 MPa range to the $PbTiO_3$ compacts in the Bridgman anvils, we manipulated with the concentration of structural defects, as it has been evidenced by changes in the values of characteristic parameters such as unit cell lengths and the size of the coherent scattering regions. The lattice was assessed by calculating the root-mean-square amplitude, the Debye characteristic temperature and the Debye–Waller factor. All of them exhibiting oscillations in values responding to the applied strain. The experimental part has been completed with vibrational and dielectric spectroscopies. For the first time a robust ferroelectric ceramic has been obtained from mechanically activated $PbTiO_3$ powder, which usually degrades at normal conditions unless being chemically doped.

Acknowledgments

The authors would like to thank Konstantin Charykov for the FTIR measurements.

Disclosure statement

No potential conflict of interest was reported by the authors.

Funding

The authors would like to acknowledge Southern Federal University for the financial support from the Grant (VnGr-07/2017-08).

ORCID iDs

K G Abdulvakhidov https://orcid.org/0000-0001-6697-9192

References

[1] Zhang R, Jiang B and Cao W 2001 Elastic, piezoelectric, and dielectric properties of multidomain $^{0.67}Pb(Mg_{1/3}Nb_{2/3})O_3$–$^{0.33}PbTiO_3$ single crystals *J. Appl. Phys.* **90** 3471–5

[2] Topolov V Yu 2013 Effect of a tetragonal phase on heterophase states in perovskite-type ferroelectric solid solutions *Solid State Commun.* **170** 1–5

[3] Uršič H, Santo Zarnik M and Kosec M 2011 $Pb(Mg_{1/3}Nb_{2/3})O_3$–$PbTiO_3$ (PMN-PT) material for actuator applications *Smart Mater. Res.* **2011** 452901

[4] Algueró M *et al* 2006 Processing by mechanosynthesis and properties of piezoelectric $Pb(Mg_{1/3}Nb_{2/3})O_3$–$PbTiO_3$ with different compositions *Acta Mater.* **54** 501–11

[5] Jaffe B, Cook W R and Jaffe H 1971 *Piezoelectric Ceramics* (New York: Academic)

[6] Smazhevskaya E G and Feldman N B 1971 *Piezoceramics* (Moscow: Sovetskoye Radio) (in Russian)

[7] Fesenko E G 1972 *Perovskite Family and Ferroelectricity* (Moscow: Atomizdat) (in Russian)

[8] Cox D E, Noheda B, Shirane G, Uesu Y, Fujishiro K and Yamada Y 2001 Universal phase diagram for high-piezoelectric perovskite systems *Appl. Phys. Lett.* **79** 400–2

[9] Guo Y and Luo H 2002 Effect of composition and poling field on the properties and ferroelectric phase-stability of $Pb(Mg_{1/3}Nb_{2/3})O_3$–$PbTiO_3$ crystals *J. Appl. Phys.* **92** 6134–8

[10] Bondarenko E I *et al* 1988 Self-destruction of ferriceramics *Sov. Phys. Tech. Phys.* **33** 1071

[11] Sirota M A *et al* 2018 Mechanical activation and physical properties of $Pb(Zr_{0.56}Ti_{0.44})O_3$ *Ferroelectrics* **526** 1–8

[12] Abdulvakhidov K G *et al* 2008 Properties of the ferroelectric ceramics $PbSc_{0.5}Ta_{0.5}O_3$ fabricated from an ultradispersed powder *Tech. Phys.* **53** 661–3

[13] Ubushaeva E N *et al* 2010 Nanostructured multiferroic $PbFe_{0.5}Nb_{0.5}O_3$ and its physical properties *Tech. Phys.* **55** 1596–9

[14] Abdulvakhidov K G *et al* 2016 Phase transitions, magnetic and dielectric properties of $PbFe_{0.5}Nb_{0.5}O_3$ *Ferroelectrics* **494** 182–91

[15] Sirota M A and Abdulvakhidov K G 2017 Mechanical activation and electrophysical properties of $Pb(Zr_{0.58}Ti_{0.42})O_3$ *J. Surf. Invest.* **11** 677–9

[16] Kraus W and Nolze G 1996 POWDER CELL—a program for the representation and manipulation of crystal structures and calculation of the resulting x-ray powder patterns *J. Appl. Cryst.* **29** 301–3

[17] Okazaki K 1969 *Ceramic Engineering for Dielectrics* (Tokyo: Gakken-sha)

[18] Vasil'ev D M and Smirnov B I 1961 Certain x-ray diffraction methods of investigating cold worked metals *Sov. Phys. Usp.* **4** 226

[19] Abdulvakhidov K G *et al* 2016 Nanostructured $SmFeO_3$ electrophysical properties *IOP Conf. Ser.: Mater. Sci. Eng.* **112** 012020

[20] Umanski YaS 1969 *X-ray Investigation of Metals and Semiconductors* (Moscow: Metallurgia) (in Russian)

[21] Gorelik S S 1978 *Recrystallization of Metals and Alloys* (Moscow: Metallurgia) (in Russian)

[22] James R W 1962 *The Optical Principles of The Diffraction of X-Rays* (London: G Bells & Sons)

[23] Last J T 1957 Infrared-absorption studies on barium titanate and related materials *Phys. Rev.* **105** 1740–50